



# Fundamental analysis of the interaction between overburden behaviour and snook stability in coalmines

by J.N. van der Merwe\*

## Synopsis

In the process of pillar extraction, pillars are seldom if ever extracted completely. The pillar remnants, or snooks, play an important role in the extraction process. At the working face, they need to be stable to provide a measure of support in the immediate area. Further back, they have to fail in a controlled manner to prevent undue load build-up on the pillars that have not yet been extracted. The stability condition at the working area is the result of interaction between the stability of the pillar and that of the roof rock.

It is shown that the primary mode of roof layer failure is by bending induced tension. Direct tension can be excluded in most practical conditions, and only in exceptional cases will the first failure be in shear mode. Panel spans required to cause the first goaf to be formed, predicted using analytical considerations, are of the same order as has been observed in practice.

Once the first goaf has formed, the horizontal stress is reduced and failure will occur at more frequent intervals. It is shown that bending induced tension is the most likely mode of failure in an unjointed roof layer. In roof layers with a high frequency of weak or uncemented jointing, failure can be expected to occur at spans equal to the joint spacing. In this context, failure will occur at the smallest of the spans required to induce tensile roof failure and the joint spacing.

A fundamental procedure to evaluate the likely roof layer failure in a stacked beam system is developed. This can be used to estimate the loading condition on snooks.

It is shown that snooks assist in stabilizing the immediate roof beam. The sizes and positions of the snooks relative to the position of the next pillar to be stooped, control the magnitude of the contribution to stability. The further the snook is from the next pillar, and the larger it is, the greater the contribution to the stability of the immediate roof.

Under the condition of loading by the immediate, continuous roof beam, the position and size of a single snook controls the load acting on it. The closer it is to the nearest solid, provided that the roof overhang extends beyond the snook, the greater the load on it. However, once the immediate roof beam fails, the loading conditions change. The snook is then loaded by the tributary area load.

A procedure is developed to assess the condition of snooks for different situations. Using the fundamental considerations developed in this paper, snooks can be designed to be stable during the active mining phase in their immediate vicinity, but to fail once the next line of pillars has been extracted.

## Introduction

The application of high-extraction coal mining methods in the absence of support for the overburden in the mined areas, as is commonly practised in South Africa, invariably results in the formation of a goaf. Knowledge of when and how the goaf forms, how high it extends and what happens to the rock layers overlying the goaf, is necessary in order to understand the rock mechanics aspects of high-extraction mining. This includes the stress build-up on surrounding pillars.

It is also necessary to be able to quantify the load acting on the snooks. In the immediate vicinity of the pillar in the process of being extracted, the snooks should be stable enough to provide at least some temporary support to the roof. Further back, however, they should fail in a controlled manner to prevent excessive load build-up on the unmined pillars.

It is important to understand goaf behaviour in order to predict when the overburden is likely to fail, to protect underground workers.

This paper describes the development of an analytical model for overburden behaviour where high extraction mining is practised. It is based on very simple fundamental concepts and tested against observations in the field.

## Observations

In this section, some observations made over several years in different coalmines in South Africa, which are of use in the development of the analytical method to evaluate snook stability and the condition of the overburden rock layers, are summarized.

\* University of Pretoria, Mineral Science Building, Pretoria, South Africa.

© The South African Institute of Mining and Metallurgy, 2005. SA ISSN 0038-223X/3.00 + 0.00. Paper received May 2004; revised paper received Dec. 2004.

# Fundamental analysis of the interaction between overburden behaviour

It is known that when pillar extraction is done, the stress regime changes in the sense that the vertical stress is relieved directly above and below the mined area and that it increases on the abutments surrounding the mined area. This includes the pillars that have not yet been extracted.

In the absence of support, the rock immediately above the pillar extracted area is likely to fail and usually does, the height of the failure being a function of the local geology (thickness and strength of the rock layers) and the mining dimensions (panel width, panel length and mining height).

In the case of high-extraction mining, where the lateral panel dimensions are several tens of metres and the mining height of the order of 1.5 to 4.0 metres, there are usually severe roof falls in the initial stages of pillar extraction, followed by a major collapse accompanied by the first occurrence of subsidence. This usually occurs at the stage when the panel advance is approximately equal to the panel width. In practical terms, this translates to a mined area of approximately 100 m to 150 m.

Subsidence observations indicated that the subsided area lags the mining face by a certain distance. Using this lag distance, it has been estimated that the angle between the face position underground and the edge of the subsided area on the surface (the goaf angle) during the active mining phase is approximately 30° to 45°, overhanging the goaf, and approximately 15° over the goaf once it has stabilized after the cessation of mining.

In the following sections, the analytical procedure will be developed. The first step will be to determine the most likely mode of roof failure. This will be used later in the development of the design procedure.

Following that, expressions will be developed to determine the conditions under which the first and subsequent failures of the overlying rock layers will occur. This will be followed by the determination of the load on snooks in different positions and of various sizes, and the contribution of the snooks to the stability of the overburden layers.

Finally, a worked example is provided to illustrate the use of the procedure.

## Mode of overburden failure

There are three possible fundamental modes of overburden failure. The overburden rock can firstly fail in pure tension, which will happen when the weight of the suspended rock is greater than the tensile strength of the rock or the tensile strength across a bedding plane.

The second potential failure mode is by induced tension at the edges of the plate. This will happen when the mathematical sum of the induced tension and the compressive horizontal stress is greater than the tensile strength of the rock.

The third possible mode is by sliding of the rock blocks along pre-existing vertical or near vertical joint planes. This will happen when the weight of the block exceeds the cohesion and frictional resistance of the joint planes.

Each of these possible modes will now be examined and the most likely one identified.

## Tensile failure

The weight of a column of rock  $t$  metres thick of square cross-section  $A$  is

$$w = At\rho g, \quad [1]$$

where  $\rho$  is the density of the rock and  $g$  the gravitational acceleration.

The tensile stress it induces on the next length is

$$\sigma_{ti} = t\rho g. \quad [2]$$

Failure will occur when  $\sigma_{ti} > \sigma_t$ , where  $\sigma_t$  is the tensile strength of the rock, or when

$$t\rho g > \sigma_t, \quad [3]$$

implying that the minimum thickness of a rock unit resulting in failure due to pure tension is

$$t = \frac{\sigma_t}{\rho g}. \quad [4]$$

According to van der Merwe and Madden (2002), the tensile strength of sedimentary rocks is in the range 5–6 MPa and the density is 2 500 kg/m<sup>3</sup>. In general, then, tensile failure can occur only if the thickness of the rock layer is greater than 200–240 m. This is thus an unlikely failure mode in intact, massive rock, and tensile failure is much more likely to occur across bedding planes with little or no tensile strength. The important conclusion here is that lithological units can be regarded as system elements for the purposes of analysis.

## Bending induced tensile failure

It has been seen that the first goaf usually occurs when the face advance is roughly equal to the panel width. The beam analogy to simulate plate behaviour is then not valid. According to Obert and Duvall (1967), the maximum tensile stress generated in a gravity loaded plate with width equal to length, is

$$t = \frac{\sigma_t}{\rho g}. \quad [5]$$

where  $\beta$  = coefficient = 0.0513

$a_t$  = plate width

$t$  = plate thickness

Failure will occur when the induced tensile stress exceeds the sum of the tensile strength of the rock and the *in situ* horizontal stress,  $\sigma_H$ , or when

$$\sigma_{pt} > \sigma_t + \sigma_H. \quad [6]$$

Combining Equations [5] and [6] yields the following expression for the minimum span required to result in failure:

$$a_t = \sqrt{\frac{t(\sigma_t + \sigma_H)}{6\beta\rho g}}. \quad [7]$$

Once failure has occurred, the beam continuity is lost and the behaviour of the rock layers can be likened to that of a cantilever, where the maximum induced tensile stress according to Obert and Duvall (1967) is given by

# Fundamental analysis of the interaction between overburden behaviour

$$\sigma_{gt} = \frac{3\rho g a_g^2}{t} \tag{8}$$

Again, using the limit condition expressed in Equation [6], Equation [8] can be transformed to yield the following expression for the minimum span required to result in failure:

$$a_{gt} = \sqrt{\frac{t\sigma_t}{3\rho g}} \tag{9}$$

Note that in Equation [9], the term  $\sigma_H$  has disappeared. This is because once the beam has failed and continuity is lost, the horizontal stress is equal to zero. Equations [7] and [9] indicate that the main variables influencing the span

required to result in goafing are the magnitude of horizontal stress and the thickness of the layers.

Note that Equations [6], [7] and [9] are valid for unjointed rock layers. If the rock is jointed, as it invariably is, the tensile strength,  $\sigma_b$  can be regarded as very small or equal to zero. Using the jointed rock condition, Figure 1 was constructed using Equation [7] to calculate the spans required to result in bending-induced tensile failure for the first goaf. The tensile strength of the rock mass was assumed to be 1 MPa.

At a depth of 100 m and  $k$ -ratio (the ratio of horizontal to vertical stress) of 2.0, the horizontal stress is 5 Mpa. Figure 1 indicates that at a horizontal stress of 5 MPa, failure will occur at a span of approximately 140 m for a 30 m thick

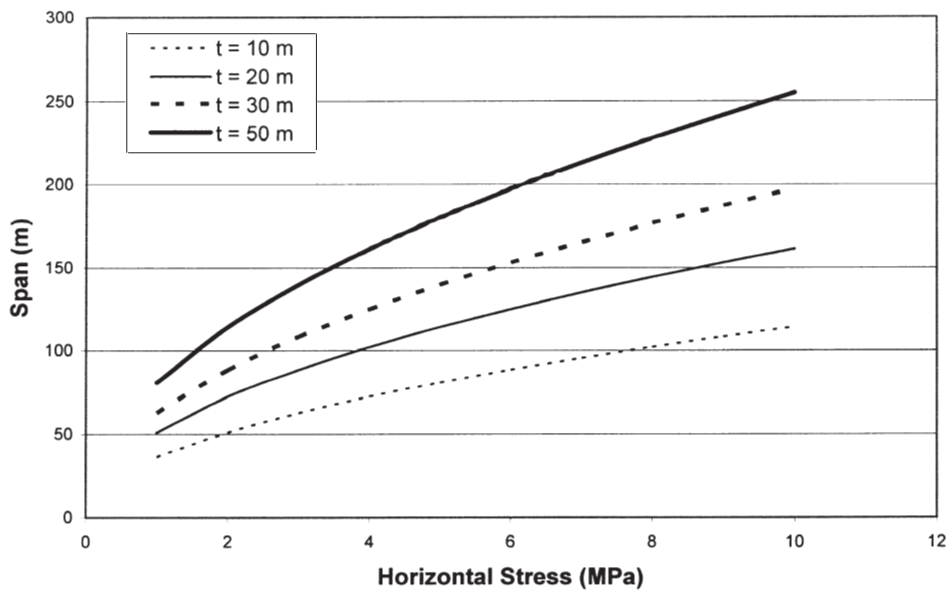


Figure 1—Minimum span required to result in bending-induced tensile failure of jointed overburden plates in the situation where the goaf has not yet been established

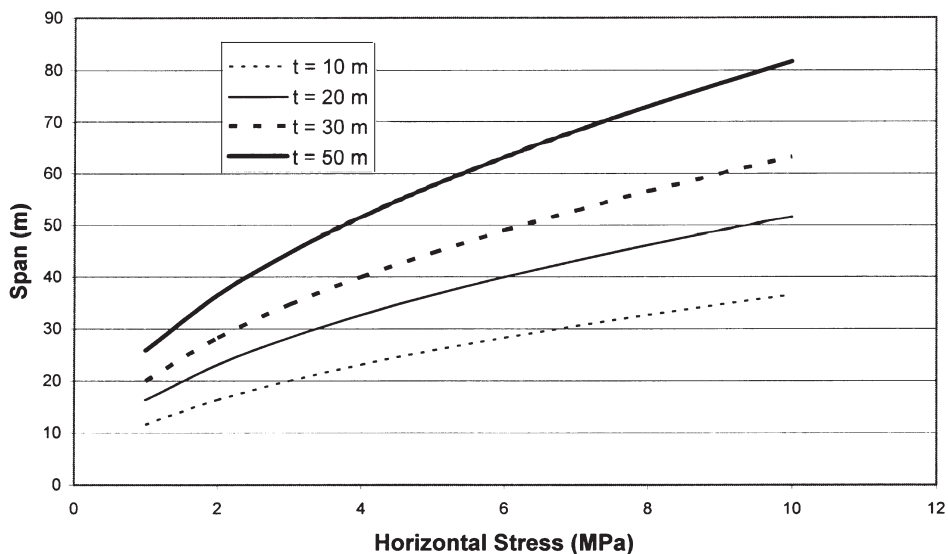


Figure 2—Minimum span required to result in bending-induced tensile failure of jointed overburden plates in the situation where the goaf has already formed

# Fundamental analysis of the interaction between overburden behaviour

layer. This is in accord with underground observations at a depth of 100 m. For a 50 m thick layer, the minimum required span increases to 180 m.

Once the goaf has formed, Equation [9] can be used to determine the minimum span required to result in further failure. Figure 2 demonstrates the minimum spans for different thickness of layers.

Comparison of Figures 1 and 2 shows that once the first goaf has formed, significantly smaller spans (or overhangs) are required for continued overburden layer failure.

## Shear failure

In the absence of additional loading on a block, sliding will occur if the weight of a block exceeds the frictional resistance forces, see Figure 3.

The weight of the block,  $W$ , is

$$W = atL\rho g \quad [10]$$

As the block is in contact with others on four sides, the resisting force,  $F_R$ , is

$$F_R = 2F_{RL} + 2F_{Rd} \quad [11]$$

or

$$F_R = 2Lt(\sigma_{HL} \tan \phi + C) + 2at(\sigma_{Ha} \tan \phi + C) \quad [12]$$

where  $\sigma_{HL}$  = horizontal stress acting across the sliding surfaces  $a-t$

$\sigma_{Ha}$  = horizontal stress acting across the sliding surfaces  $L-t$

$\phi$  = angle of friction

$C$  = cohesion

$L$ ,  $t$  and  $a$  = dimensions of the block, shown in Figure 3.

If the simplifying assumption that  $\sigma_{HL} = \sigma_{Ha} = \sigma_H$  is made, Equation [12] can be simplified to

$$F_R = 2t(L + a)[\sigma_H \tan \phi + C] \quad [13]$$

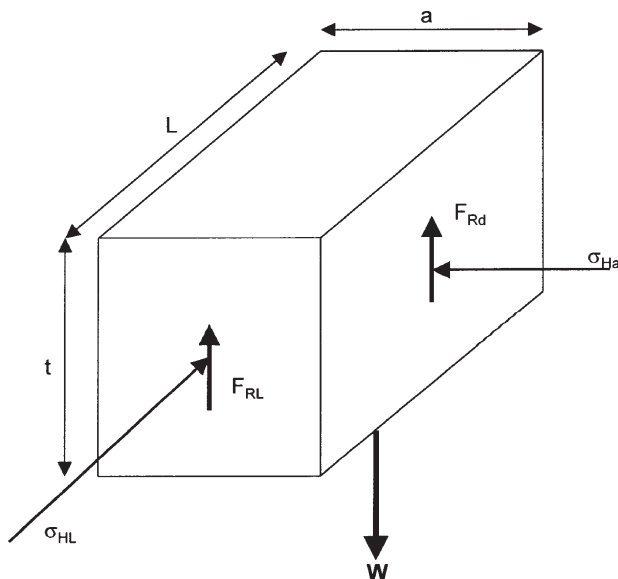


Figure 3—Diagram illustrating sliding failure of a block between other blocks

Failure will occur if  $W > F_R$ , or

$$\frac{La}{L + a} > \frac{2(\sigma_H \tan \phi + C)}{\rho g} \quad [14]$$

Introducing, for the purposes of demonstration, the further simplification that the joint spacing is equal in all directions, or that  $L = a = a_s$ , Equation [14] can be further simplified to yield the maximum spacing prior to failure

$$a_s = \frac{4(\sigma_H \tan \phi + C)}{\rho g} \quad [15]$$

Once the goaf has formed, the horizontal stress in one direction will disappear and the problem can be simplified to two dimensions. Then the resisting force at equilibrium,  $F_r$ , is

$$F_r = 2Lt[\sigma_H \tan \phi + C] \quad [16]$$

Failure will occur if  $W > F_r$ , or the minimum value of  $L$  is

$$L = \frac{2[\sigma_H \tan \phi + C]}{\rho g} \quad [17]$$

The required value of  $L$  in Equation [17] is half of that of  $a_s$  in Equation [15], indicating that once the goaf has formed, it propagates more easily. It is also clear that the layer thickness does not play a role in the consideration of failure due to shear stress.

For a first-order quantification to investigate the validity of the concept, values of  $\phi$  and  $C$  for joints in sandstone, shale and dolerite as shown in Table I were chosen.

Equations [15] and [17] were used to construct curves for the minimum span required to result in shear failure for different values of horizontal stress, shown in Figure 4.

Figure 4 shows that the span required for shear failure of rock under its own weight at a horizontal stress of 5 Mpa (i.e. 100 m depth with a  $k$ -ratio of 2.0) is in excess of 600 m. This is not consistent with observation in practice, where the first goaf at a depth of 100 m usually occurs at a span of 100–150 m.

## Comparison of failure modes

It has been shown that pure tension can be excluded as a likely failure mode for the overburden rock mass. The rest of the discussion is thus devoted to a comparison of shear failure and failure caused by induced tension due to plate deflection.

Table I

### Values of $\phi$ and $C$ for a first-order validity check

Rock type	$\phi$	$C$ (kPa)
Sandstone (before goaf) <sup>1</sup>	35°	300
Sandstone (after goaf) <sup>1</sup>	35°	50
Shale (before goaf) <sup>1</sup>	28°	800
Shale (after goaf) <sup>1</sup>	28°	200
Dolerite (before goaf) <sup>2</sup>	35°	500
Dolerite (after goaf) <sup>2</sup>	35°	100

<sup>1</sup>van Schalkwyk, 2003

<sup>2</sup>Terbrugge, 1994

# Fundamental analysis of the interaction between overburden behaviour

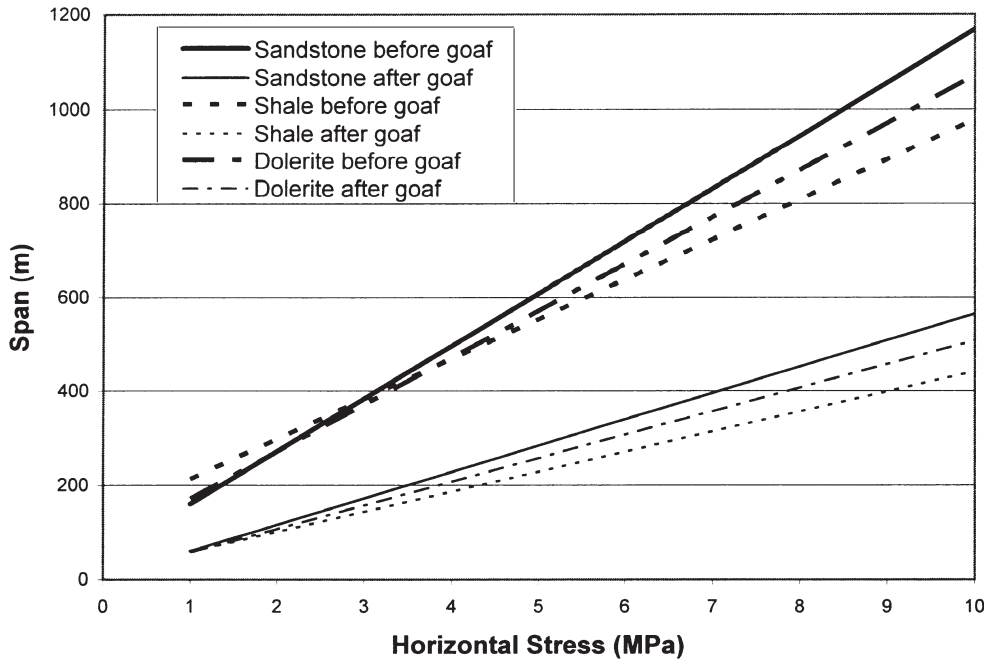


Figure 4—Span required for shear failure as a function of horizontal stress

As the rock layers are seldom of uniform thickness, it is to be expected that loading of the blocks or plates will not necessarily be pure gravity loading, but that upper layers could add to the loading of the bottom layers.

The span required to result in failure is not affected equally by additional loading in the cases of shear and tensile failure. Scrutiny of Equations [7], [9], [15] and [17] indicates that, in the cases of shear failure, the required span is proportional to the inverse of the additional load, while in the case of tensile failure, it is proportional to the inverse of the square root of the additional load.

In the case of tensile failure, the span required to result in the first goaf where additional loading by a rock layer of thickness  $\delta t$  is present, can be obtained by the more complete expression

$$a_t = \sqrt{\frac{t^2(\sigma_t + \sigma_H)}{6\beta\rho g(t + \delta t)}} \quad [18]$$

and the equivalent expression for shear failure is then

$$a_s = \frac{4t(\sigma_H \tan \phi + C)}{\rho g(t + \delta t)} \quad [19]$$

From Equations [18] and [19],

$$\frac{a_t}{a_s} = \sqrt{\frac{t^2(\sigma_t + \sigma_H)}{6\beta\rho g(t + \delta t)}} \frac{\rho g(t + \delta t)}{4t(\sigma_H \tan \phi + C)} \quad [20]$$

or, with the simplifying assumption that the cohesion and tensile strength are equal to zero, or  $C = \sigma_t = 0$

$$\frac{a_t}{a_s} = \frac{\sqrt{\rho g / 6\beta}}{4 \tan \phi} \sqrt{\frac{t + \delta t}{\sigma_H}} \quad [21]$$

For values of  $\rho g = .025 \text{ MN/m}^3$ ,  $\beta = 0.0513$  and  $\phi = 28^\circ$  (i.e. shale), Equation [20] can be simplified to

$$\frac{a_t}{a_s} = 0.134 \sqrt{\frac{t + \delta t}{\sigma_H}} \quad [22]$$

and for sandstone, with  $\phi = 35^\circ$ ,

$$\frac{a_t}{a_s} = 0.102 \sqrt{\frac{t + \delta t}{\sigma_H}} \quad [23]$$

For the span required for bending-induced tensile failure to be greater than that for shear failure ( $a_t/a_s > 1$ ), in other words, for shear failure to occur before bending-induced tensile failure, the condition

$$t + \delta t > 55.7\sigma_H \text{ for sandstone and} \quad [24]$$

$$t + \delta t > 96.1\sigma_H \text{ for shale} \quad [25]$$

must be satisfied (note that the stress units here are in MPa).

The thickness of rock layers is usually of the order of 5 m to 30 m and the horizontal stress is of the order of 1 to 10 MPa, leading to the conclusion that, only in exceptional cases, will the span required for shear failure be less than that required for induced tensile failure.

For instance, the simplified Equation [24] can also be written in the form

$$t + \delta t > 55.7(k\sigma_v), \quad [26]$$

or

$$t + \delta t > 55.7(k\rho gH), \quad [27]$$

and as the term  $t + \delta t$  can never be greater than  $H$ , because the total thickness of the overburden rock layers cannot be greater than the depth, it follows that

$$k < \frac{1}{55.7\rho g} = 0.72, \quad [28]$$

# Fundamental analysis of the interaction between overburden behaviour

indicating that shear failure can only occur before tensile failure for the described typical situations if the ratio of horizontal to vertical stress is less than 0.72. The  $k$ -ratio at shallow depth is usually greater than 1.0.

It can therefore be concluded that the predominant failure mode of the overburden rock layers is tensile failure induced by bending of the layers.

## Conditions for failure of rock layers

As it has been shown above, that bending-induced tension is the most likely failure mode, this is the mode that will be considered further. The overburden strata in a sedimentary environment is layered, consisting of layers of different thickness and stiffness. The analytical model best suited to this environment is that of composite plates, simplified to composite beams. The necessary assumption to validate this simplification is that the length of the plate must be greater than twice its width, or that the face advance must be greater than twice the panel width.

The first goaf, which often occurs when the face advance is equal to the panel width, will be treated as a special case as the simplification is obviously then not valid. The analogy for that case will be that of a square plate.

## First goaf

### Induced tensile stress in layers

The first goaf will occur when the induced tensile stress in the rock layers (analogous to plates) exceeds the tensile strength of the rock—or the tensile strength across a joint—plus the horizontal stress. For this, Equation [5] is used in a slightly expanded form to incorporate the additional loading from upper rock layers. Then, the induced tensile stress at the edge of the plate is

$$\sigma_{pt} = \frac{6\beta\rho g T a_i^2}{t^2} \quad [29]$$

where  $T$  = total thickness of layer under consideration plus all layers adding additional loading  
 $t$  = thickness of layer under consideration.

Upper layers will contribute to the loading of bottom beams if the potential for deflection exceeds that of the bottom layer. Here a further simplification is introduced:

It is assumed that if upper layers load the bottom layers, the additional load will be the full weight of the upper layer. This is valid in a rock environment where the elastic range is small in the tensile stress regime and layers are prone to failure.

### Tensile resisting stress

The tensile strength of the rock mass is very low, given the jointed nature of the rock mass. It can be regarded as being between 0 and 1 MPa. The relative contribution of horizontal stress therefore increases, and some discussion of it is required.

Stacey and Wesseloo (1998) reviewed the measured in situ rock stress data in South Africa. Figure 5 has been constructed from data in their report, showing the  $k$ -ratio ( $k$  being the ratio between horizontal and vertical stress) as a function of depth.

It is seen that the  $k$ -ratio clusters around a value of approximately 0.8 at greater depth, while the scatter increases at shallow depth where much higher values are apparent. The information has been used to back calculate values for horizontal stress, shown in Figure 6.

Further investigation of the data for shallow depth (less than 300 m) resulted in the data shown in Figure 7.

Figure 7 indicates that the  $k$ -ratio at shallow depth is approximately 2, as the vertical stress is equal to  $0.025 H$ . The scatter in the data also indicates the difficulty inherent in obtaining reliable stress measurement results at shallow depth. This is due to the measurement techniques, based on the relaxation of rock when it is destressed. In a low-stress environment, the expansion of unloaded rock specimens is small and it is difficult to measure the small magnitudes of expansion accurately.

Figure 8 was therefore constructed, by merely replacing the individual data points by the average stresses obtained at the different depths.

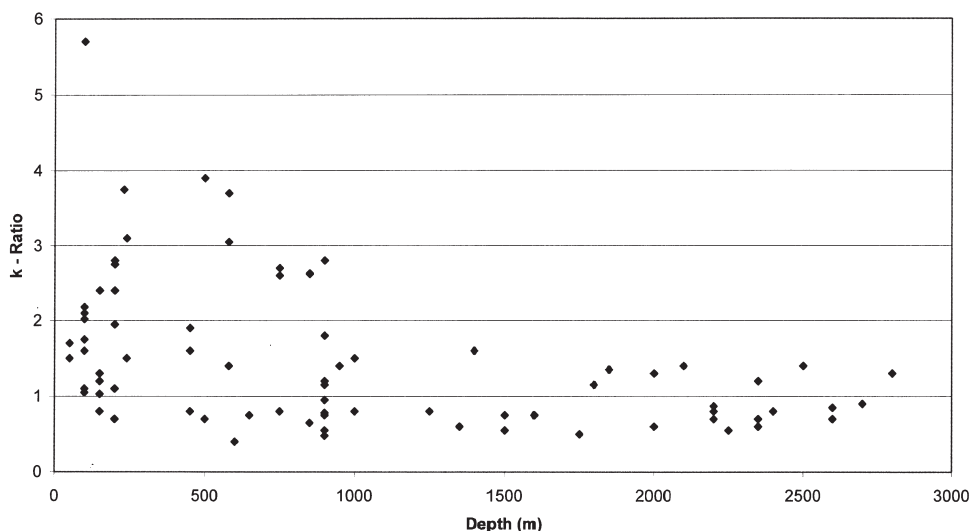


Figure 5—The relationship between the  $k$ -ratio and depth, after Stacey and Wesseloo (1998)

# Fundamental analysis of the interaction between overburden behaviour

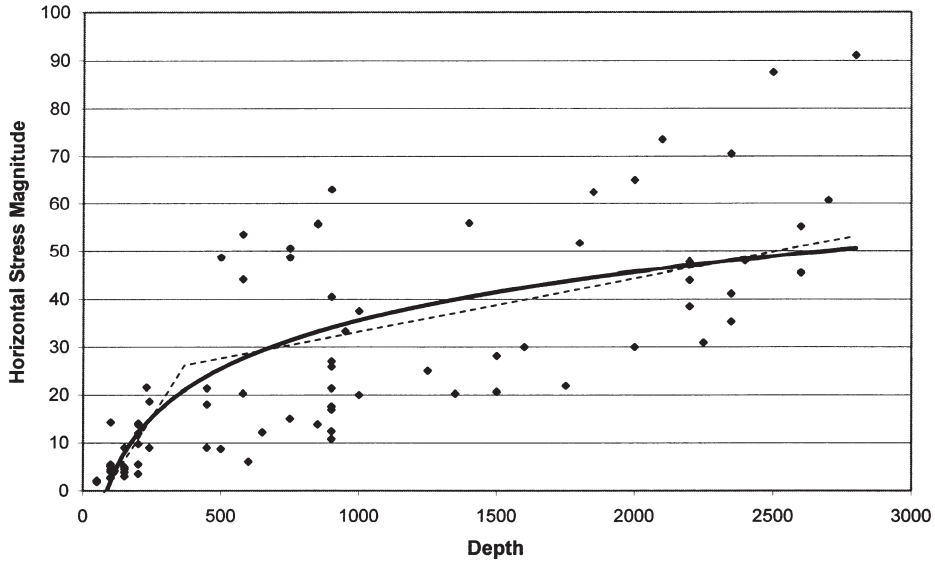


Figure 6—Horizontal stress as a function of depth. The logarithmic trend line has been approximated as a bi-linear trend, shown as the broken line in the figure

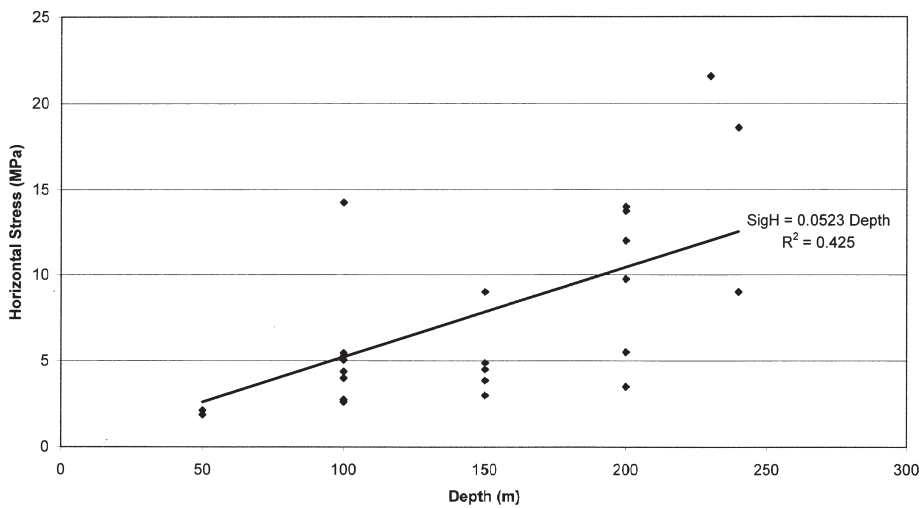


Figure 7—Magnitude of horizontal stress vs. depth for depth less than 300 m. Note the scatter, resulting in a low correlation coefficient between the trend line and the data

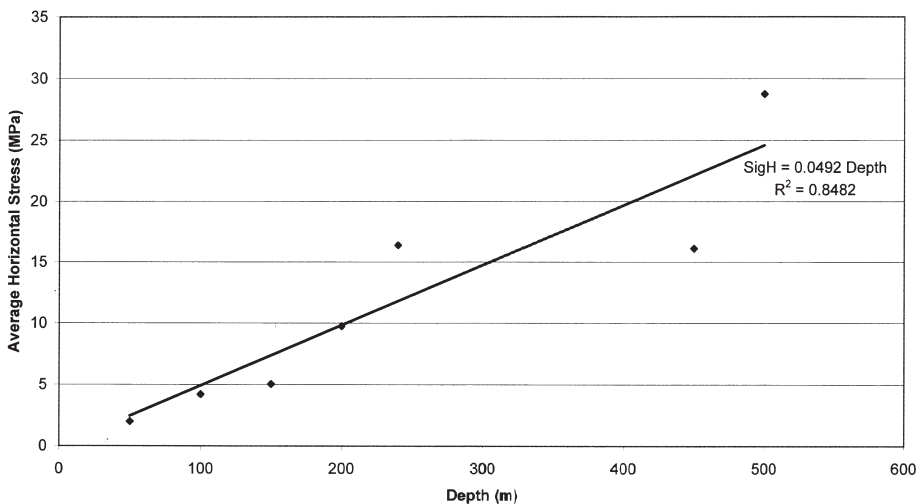


Figure 8—Average magnitude of horizontal stress vs depth for depth less than 300 m

## Fundamental analysis of the interaction between overburden behaviour

The scatter of the data has now been significantly reduced. The expression for the magnitude of horizontal stress is then

$$\sigma_H = 0.49H, \quad [30]$$

which indicates that at shallow depth, the  $k$ -ratio can be taken as approximately 2.0, with the cautionary note that there is significant variability as shown by Figure 7.

The total stress that will resist bending-induced tensile failure can now be written as

$$\sigma_{tr} = .049H + \sigma_t \quad [31]$$

### First goaf

For the first failure to occur, Equation [18] can be used to calculate the required span, which is the panel width required to result in overburden failure. Substituting Equation [30] into [18] and .0513 for  $\beta$ , results in the following equation to calculate that span,  $a_{fg}$ :

$$a_{fg} = \sqrt{\frac{t^2(\sigma_t + .049H)}{.3078\rho g(T)}} \quad [32]$$

For the purposes of predicting whether the overburden will collapse or not for a given panel width, Equation [32] is used to calculate the minimum span required to result in failure. If that is greater than the given panel width, failure will not occur and vice versa.

The calculation procedure consists of several iterations to determine  $T$  for each layer. In the first iteration,  $a_{fg}$  is calculated for each layer individually, without any additional loading. The thickness of each layer where the effective panel width is greater than  $a_{fg}$ , is added to the thickness of the layer underneath. This is a cumulative process ending each

time at the layers with  $a_{fg}$  greater than the effective panel width. The next iteration consists of the recalculation of  $a_{fg}$  for the surviving layers. The process continues until all the possible failures have been evaluated. Care should be taken to use the appropriate density for each layer—this is especially important where the much denser dolerite sill is present in the overburden.

The effective panel width,  $W_e$ , for each layer is the physical panel width minus the overhang of the layer immediately beneath it, or

$$W_e = W - 2H_B \tan \theta \quad [33]$$

where  $W$  = physical panel width

$H_B$  = parting between coal-seam floor and base of layer under consideration

$\theta$  = goaf angle, commonly  $30^\circ$  to  $45^\circ$ .

### Subsequent goafing

Once the initial goaf has formed and the overburden plates have lost continuity, the plate analogy is no longer valid. The analysis is then simplified, as the analogy now is that of cantilevers with varying thickness and loading conditions. Due to the loss of continuity of the plates, the horizontal stress is zero.

The very basic equation for maximum tensile stress in a cantilever with a uniformly distributed load, in this case the weight of the rock layer plus the weight of upper layers contributing to its load, is

$$\sigma = \frac{3\rho g T a^2}{t^2} \quad [34]$$

If the length of overhang at equilibrium is denoted by  $a_o$ , it follows that

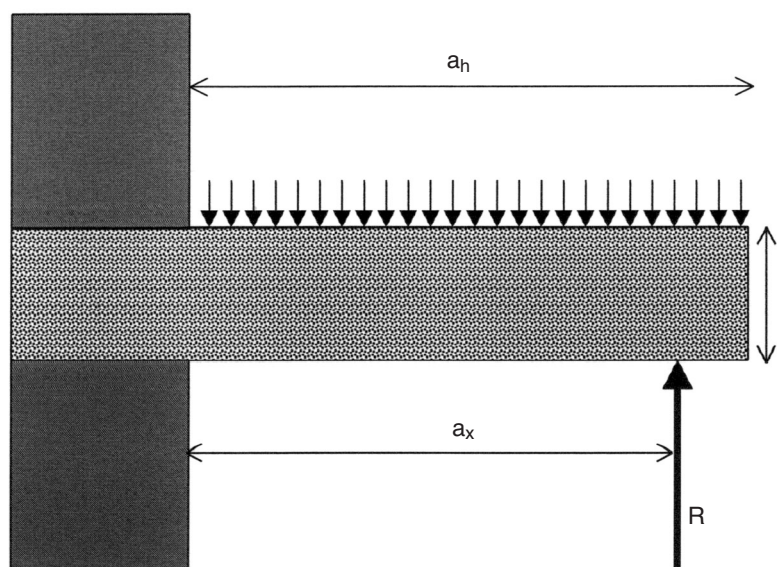


Figure 9—Conceptual model for an overhang of length  $a_h$  supported by a snook offering resistance  $R$  at a distance  $a_x$  from the closest solid pillar



## Fundamental analysis of the interaction between overburden behaviour

$$a_o = 0.58t \sqrt{\frac{\sigma_t}{\rho g T}} \quad [35]$$

An important issue is whether to substitute the intact material tensile strength for  $\sigma_t$  in Equation [35] or whether to use a much lower value for the tensile strength across joints. There is no clear-cut answer to this question as it depends primarily on the joint condition.

Consider, as an example, the situation where alternating layers of sandstone and shale, each 5 m thick, make up the overburden rock. Then,  $T = 10$ ,  $t = 5$  and  $\rho g = .025 \text{ MN/m}^3$  in Equation [34]. For intact sandstone, with  $\sigma_t = 5 \text{ MPa}$ ,  $a_o$  is equal to 13 m. If the joint spacing is sufficiently greater than 13 m for the end of the rock layer to be clamped effectively, then failure will occur when the face has advanced 13 m. If it is less than that, then failure will occur when the advance is equal to the joint spacing, under the reasonable assumption that the tensile strength across a joint is zero.

### Interaction between pillars and overhang during stooping

#### Effects on overhang

The discussion above is valid for the case where there is no support for the cantilevers making up the overburden strata, as in longwalling. In pillar extraction, this is not the case, as there are invariably snooks of different sizes. A more appropriate analogy for this case is that of a cantilever with uniformly distributed load and a point support underneath. This is conceptually shown in Figure 9.

The generic expression for the maximum induced tensile stress in a rectangular beam of width  $b$  and thickness  $t$  is

$$\sigma = \frac{6M}{bt} \quad [36]$$

where  $M$  is the moment about the clamped end of the beam.

For the situation as shown in Figure 8, the moment is:

$$M = \frac{a_h^2 q}{2} - R a_x \quad [37]$$

where  $q$  is the uniformly distributed load on the beam, equal to  $b\rho gT$ .

#### The resistance $R$ offered by the snook

The value of  $R$  depends on whether the overhanging beam is intact or failed, and on whether the snook is itself in a failed or intact state. In the following discussion, the reaction of the snook under different situations is denoted by  $F_x$ —the appropriate value will be equated to  $R$  in Equation [37].

If the overhanging beam is intact,  $F_{xi}$  is found by following the procedure for determining the reaction in the case of a statically indeterminate beam, by balancing the displacements at the position of the force. This procedure is described in several handbooks, such as Morley (1943).

The value of  $F_{xi}$  in terms of the symbols used in this paper is then found to be

$$F_{xi} = \frac{3q}{2} \left( \frac{1}{2} \frac{a_h^2}{a_x} - \frac{1}{3} a_h + \frac{1}{12} a_x \right) \quad [38]$$

If the snook is situated at the far end of the overhang, i.e.  $a_x = a_h$ , the equation can be simplified to

$$F_{xi} = \frac{3qa_h}{8} \quad [39]$$

If the overhanging beam has failed, the load on the snook,  $F_{xf}$ , is the dead weight of the overhang, or

$$F_{xf} = \rho g T b \quad [40]$$

Equation [39] only remains valid for as long as the snook does not fail. Once it does,  $F_x$  becomes zero. There is thus an upper limit to the value of  $F_x$ , denoted  $F_{xm}$ . According to van der Merwe (2003), the strength of a coal pillar in stress units is

$$\sigma = 3.5 \frac{w}{h}, \text{ (MPa)} \quad [41]$$

where  $h$  is the pillar height and  $w$  the pillar width.

In this case, the units to be used are those for a force, thus the strength of a pillar becomes

$$F_{xm} = 3.5 \frac{w^3}{h} \text{ (MN)} \quad [42]$$

Substitution of Equation [38] and [37] into [36] yields the following single expression for the tensile stress generated in an overhang beam,  $\sigma_{si}$ , provided the snook is intact:

$$\sigma_{si} = \frac{q}{3bt} \left[ a_h a_x - \frac{a_h^2}{2} - \frac{a_x^2}{4} \right] \quad [43]$$

Once the snook has failed, the expression becomes

$$\sigma_{sf} = \frac{3a_h^2 q}{bt} \quad [44]$$

To summarize, the value of  $R$  in Equation [37] is as determined by Equation [38] if the overhanging beam is intact. If the resistance found by Equation [38] exceeds the limiting condition given by Equation [42],  $R = 0$ .

The procedure requires iteration, as the condition of the overhanging beam is a function of the magnitude of induced tension, found with Equation [36], which requires  $R$  as an input variable. In most cases, however, it will be found that as long as the snook strength given by Equation [42] exceeds the load on it according to Equation [38], the overhang will also be stable.

#### Example

The following simple example is provided to clarify the procedures described in the preceding paragraphs.

# Fundamental analysis of the interaction between overburden behaviour

In stooping, it is important for a snook to be stable in the immediate working area, but to fail once stooping has advanced to the next line of pillars. Consider the following situation:

Stooping is done in a panel with 24 m pillar centres and 6 m road width at 3 m mining height. Snooks are left on the four corners of the pillars. The last snook, i.e. the one closest to the next solid pillar (see Figure 10) is the largest. The other snooks are significantly smaller.

The roof consists of a 3 m thick stiff, competent sandstone overlain by 17 m of softer mudstone. Find the size of snook that will be stable during the time that mining is done in its vicinity, but that will fail once the next line of pillars are extracted.

The following values can be assigned to the various parameters:

$$b = 24 \text{ m}$$

$$t = 3 \text{ m}$$

$$T = 20 \text{ m}$$

$$a_h \text{ after the stooping of the first line} = 24 \text{ m}$$

$$a_h \text{ after the stooping of the second line} = 48 \text{ m}$$

$$a_x = 6 \text{ m plus half of the snook size.}$$

$$\rho = 2\,500 \text{ kg/m}^3$$

The effect of the smaller snooks can be disregarded for the purposes of the example.

The easiest way is to solve the different equations for a range of pillar sizes using a standard spreadsheet. This was done for pillars in the range 1 to 5 m wide. The results are summarized in Table II.

Using the results in Table II, Figure 10 was constructed, comparing the snooks' strength to their load for the two situations, i.e. after extraction of the first line of pillars and after the extraction of the second line of pillars.

The stabilizing role of the snooks is demonstrated by the 5th column in Table II. In the cases where the snooks have failed, a tensile stress is generated in the roof beam, indicating failure. In the cases where the snooks are intact, the stress situation remains compressive, indicating a stable roof and consequently a safe working environment.

Figure 10 indicates three zones. In the first zone, the load on the snooks less than 2.5 m wide, exceeds their strength even with mining of the first line of pillars. Those snooks will fail prematurely. At the other end, snook size greater than approximately 4.1 m, the snooks' strength exceed the load on them after mining of the second line of pillars, indicating that they will remain stable when they are required to fail. The

Table II

### Results

Pillar width (m)	Pillar Strength (MN) Eqn. [42]	Pillar Load (MN) Eqn. [38]	Resistance R (MN)	Induced Tension* (MPa) Eqn. [43]/[44]
First pillar (overhang = 24 m)				
1	1.17	23.50	0.00	10.20
2	9.33	21.51	0.00	10.20
3	31.50	19.78	19.78	-2.16
4	74.67	18.28	18.28	-1.99
5	145.83	16.96	16.96	-1.81
Second pillar (overhang = 48 m)				
1	1.17	103.14	0.00	40.80
2	9.33	95.10	0.00	40.80
3	31.50	88.13	0.00	40.80
4	74.67	82.04	0.00	40.80
5	145.83	76.66	76.66	-13.50

\* Tensile stresses are positive. A negative value indicates that the contribution of the snook results in a compressive stress at the edge of the overhang beam

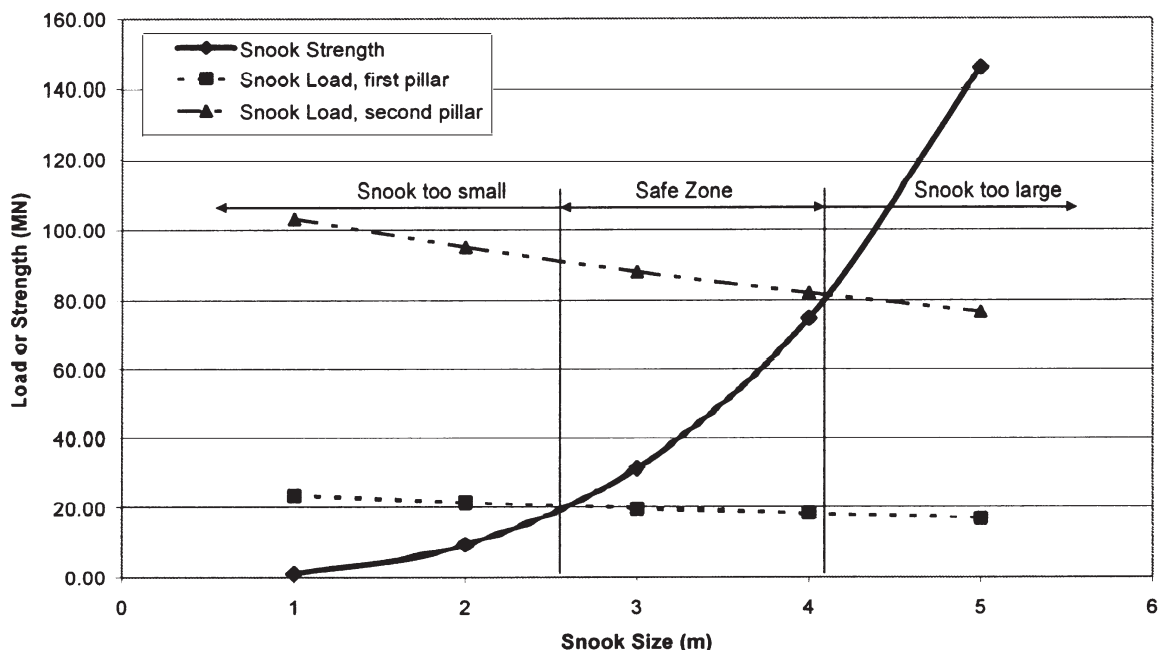


Figure 10—Comparison of the load on the snooks to their strength

# Fundamental analysis of the interaction between overburden behaviour

'Safe zone' is between these extremes, where the snooks' strength is greater than their load after mining of the first line of pillars, but less than their load after the extraction of the second line of pillars.

The optimum snook size for this example is thus in the range 2.5 m to 4 m.

## Conclusions

### Mode of goaf formation

- ▶ The primary mode of roof layer failure is by bending-induced tension. Direct tension can be excluded in most practical conditions, and only in exceptional cases will the first failure be in shear mode
- ▶ Panel spans required to cause the first goaf to be formed according to the analytical procedure, are of the same order as has been observed in practice
- ▶ Once the first goaf has formed, the horizontal stress in the goaf is reduced and failure will occur at more frequent intervals. Bending-induced tension remains the most likely mode of failure in an unjointed roof layer
- ▶ In roof layers with a high frequency of jointing, failure can be expected to occur at spans equal to the joint spacing. In this context, failure will occur at the smallest of the spans required to induce tensile roof failure and the joint spacing
- ▶ The magnitude of the horizontal stress is of great importance in both the tensile and shear failure modes.

### Role of snooks

- ▶ Snooks assist in stabilizing the immediate roof beam
- ▶ The sizes and positions of the snooks relative to the position of the next pillar to be stooped, control the magnitude of the assistance to stability. The further the snook is from the next pillar, and the larger it is, the greater the contribution to the stability of the immediate roof.

### Condition of snooks

Under the condition of loading by the immediate, continuous roof beam, the position and size of a snook controls the load acting on it. The closer it is to the nearest solid, provided that the roof overhang extends beyond the snook, the greater the load on it. However, once the immediate roof beam fails, the loading conditions change. The snook is then loaded by the much higher tributary area load.

### Snook size design

- ▶ A fundamentally based procedure has been developed to assess the condition of snooks for different situations
- ▶ The stability of the snooks depend on their size, position relative to the nearest unstooped pillar and the

condition of the immediate roof and the rest of the overburden

- ▶ The condition of the overburden and the immediate roof beam are site specific, and it would be dangerous to transfer a mining layout that depends on the stability of the snooks from one area to another without taking cognisance of changes in geological conditions
- ▶ Snooks can be designed using fundamental analytical procedures to be stable in the immediate working area and then to fail once mining progresses further. Due to the inherent variability in rock properties, this should be used only as a first order design. Refinement should follow observation
- ▶ The procedures developed in this paper should be especially helpful when existing designs require adaptation when mining conditions such as the seam thickness or pillar sizes change.

### Practical considerations

The procedure developed in this paper concentrates on the rock engineering aspects. In practice, there are several other variables that impact on pillar design, such as equipment characteristics, ventilation requirements, etc. The final design should be a combination of all the considerations. It is thus to be expected that a practical design process will undergo several iterations. A compromise, without going back to check the final design, is dangerous. The correct design is one that satisfies all the requirements, which can only be found by the various parties working together.

### Acknowledgement

The management team of the Coaltech 2020 research initiative is acknowledged for sponsoring the work and for permission to publish this paper. Mr Bill Abel of Anglo American plc is acknowledged for constructive criticism and advice.

### References

- VAN DER MERWE, J.N. New pillar strength formula for South African coal. *Journal of South African Institute of Mining and Metallurgy*, June 2003. pp. 281-292.
- VAN SCHALKWYK, A. Personal communication. 2003.
- TERBRUGGE, P. Personal communication. 1994.
- STACEY, T.R. and WESSELOO, J. Evaluation and upgrading of records of stress measurement data in the mining industry. *Safety in Mines Research Advisory Committee Report no GAP511b*. SIMPROSS, Johannesburg, South Africa. 1998.
- VAN DER MERWE, J.N. and MADDEN, B.J. *Rock Engineering for Underground Coal Mining*. South African Institute of Mining and Metallurgy Special Publications Series No 7. 2002.
- OBERT, L. and DUVALL, W.I. *Rock mechanics and the design of structures in rock*. John Wiley & Sons Inc, New York. 1967.
- MORLEY, A. *Strength of materials*. Longmans, Green and Company, London. 1943. ◆

# INTERNATIONAL ACTIVITIES

**2 0 0 5**

**6–8 January, 2005 — Mineral Processing Technology**

Dhanbad, India

Contact: Prof. R. Venugopal, Chief Coordinator (MPT-2005)

Tel: +8610-6278-9637

E-mail: ismmpt2005@yahoo.co.in

Website:

<http://www.ismdhanbad.ac.in/noticeboard/seminars.htm>

**24–28 January, 2005 — 10th ACUUS Conference - Underground Space: Economy and Environment &**

**ISRM Regional Symposium - Rock Mechanics for Underground Environment**

Moscow, Russia

Contact: Dr Olga Postolskaya, Moscow State University of Civil Engineering, Yaroslavskoye Shosse 26, 129337

Moscow, Russian Federation

Tel: +7 095 918 05 43; Fax: +7 095 261 81 88

E-mail: info@acuus-isrm05.ru

Website: [www.acuus-isrm05.ru](http://www.acuus-isrm05.ru)

**14–15 March, 2005 — Pyrometallurgy 05**

Cape Town, South Africa

Fax: +44 1326 318352

E-mail: [bwills@min-eng.com](mailto:bwills@min-eng.com)

Website: [www.min-eng.com](http://www.min-eng.com)

**15–18 March, 2005 — The design of slurry pipeline systems**

Cape Town, South Africa

Contact: Ferial Jawoodien

Tel: +27 (0) 21 683 4734; Fax: +27 (0) 21 683 4168

E-mail: [ferial@pce.co.za](mailto:ferial@pce.co.za)

**16–18 March, 2005 — Bio- & Hydrometallurgy 05**

Cape Town, South Africa

Fax: +44 1326 318352

E-mail: [bwills@min-eng.com](mailto:bwills@min-eng.com)

Website: [www.min-eng.com](http://www.min-eng.com)

**5–8 April, 2005 — MiningWorld Russia 2005**

Moscow, Russia

Contact: Mr Oleg A. Netchaev, A IDM Brand Director, MiningWorld Events

Tel: +44(0)20 7596 5213

E-mail: [oleg.netchaev@miningandevents.com](mailto:oleg.netchaev@miningandevents.com)

Mobile: +44(0)7812 019956

MiningWorld Russia - [www.miningworld-russia.com](http://www.miningworld-russia.com)

**24–27 April, 2005 — Mining Rocks**

Toronto, Canada

Website: [www.cimtoronto2005.org](http://www.cimtoronto2005.org)

**10–12 May, 2005 — Second World Conference on Sampling and Blending**

Queensland, Australia

Contact: Alison McKenzie, Senior Conference & Events Coordinator, The Australasian Institute of Mining and Metallurgy, P O Box 660, Carlton South, Victoria Australia, 3053

Tel: +61 3 9662 3166; Fax: +61 3 9662 3662

E-mail: [conference@ausimm.com.au](mailto:conference@ausimm.com.au)

Website: [www.ausimm.com](http://www.ausimm.com)

**18–20 May, 2005 — Aachen International Mining Symposia - Second Conference on SDIMI 2005 - Sustainable development indicators in the minerals industry**

Aachen, Germany

Contact: Mirjam Rosenkranz, RWTH Aachen University, Institute of Mining Engineering I, Wuellnerstraße 2 - 502062 Aachen, Germany

Tel: +49-(0)241-80-9 5673 or -9 5667

Fax: +49-(0)241-80 92-272

E-mail: [rosenkranz@bbk1.rwth-aachen.de](mailto:rosenkranz@bbk1.rwth-aachen.de)

**June, 2005 — The 19th International Mining Congress and Fair of Turkey**

Izmir, Turkey

Contact: Dr Ahmet H. Onur

E-mail: [imcet2005@imcet.org](mailto:imcet2005@imcet.org)

Website: [www.imcet.org](http://www.imcet.org)

**5–8 June, 2005 — The Third Southern African Conference on Base Metals - 'South Africa's response to changing global base metals market dynamics'**

Copper Belt, Zambia

Contact: The Conference Co-ordinator, SAIMM,

P O Box 61127, Marshalltown, 2107, South Africa

Tel: 27 11 834-1273/7; Fax: 27 11 838-5923 / 833-8156

E-mail: [sam@saimm.co.za](mailto:sam@saimm.co.za)

Website: <http://www.saimm.co.za>

**5–9 June, 2005 — Centenary of Flotation Symposium**

Brisbane, Australia

Contact: Miriam Way, Events Manager, AusIMM Central Services, The Australasian Institute of Mining and Metallurgy, P O Box 660, Carlton South, Victoria Australia,

3053

Tel: +61 3 9662 3166; Fax: +61 3 9662 3662

E-mail: [miriam@ausimm.com.au](mailto:miriam@ausimm.com.au)

<http://www.ausimm.com.au>

**13–15 June, 2005 — Processing & Disposal of Mineral Industry Wastes 05**

Falmouth, UK

Fax: +44 1326 318352

E-mail: [bwills@min-eng.com](mailto:bwills@min-eng.com)

Website: [www.min-eng.com](http://www.min-eng.com)